



# Passively Q-switched wavelength-tunable 1- $\mu\text{m}$ fiber lasers with tapered-fiber-based black phosphorus saturable absorbers

Huaqing Song<sup>a</sup>, Qi Wang<sup>a</sup>, Dongdong Wang<sup>a</sup>, Li Li<sup>a,b,\*</sup>

<sup>a</sup>School of Electronic and Optical Engineering, Nanjing University of Science and Technology, Nanjing 210094, China

<sup>b</sup>Advanced Launching Cooperation and Innovation Center, Nanjing University of Science and Technology, Nanjing 210094, China



## ARTICLE INFO

### Article history:

Received 6 September 2017

Received in revised form 8 December 2017

Accepted 9 December 2017

Available online 14 December 2017

### Keywords:

Passively Q-switched laser

Black phosphorus

Taper fiber

Ytterbium-doped fiber laser

Sagnac fiber loop

## ABSTRACT

In this paper, we demonstrated passively Q-switched wavelength-tunable 1- $\mu\text{m}$  fiber lasers utilizing few-layer black phosphorus saturable absorbers. The few-layer BP was deposited onto the tapered fibers by an optically driven process. The wavelength tunability was achieved with a fiber Sagnac loop comprised of a piece of polarization maintaining fiber and a polarization controller. Stable Q-switching laser operations were observed at wavelengths ranging from 1040.5 to 1044.6 nm at threshold pump power of 220 mW. Maximal pulse energy of 141.27 nJ at a repetition rate of 63 kHz was recorded under pump power of 445 mW.

© 2017 The Authors. Published by Elsevier B.V. This is an open access article under the CC BY-NC-ND license (<http://creativecommons.org/licenses/by-nc-nd/4.0/>).

## Introduction

Passively Q-switched fiber lasers based on saturable absorbers (SAs) have attracted substantial research attention for applications in material processing, spectroscopy, medical diagnoses, and fiber telecommunications. Semiconductor saturable absorber mirrors (SESAMs) have been adopted for most commercial applications owing to their mature manufacturing processes [1]. However, disadvantages of SESAMs such as complicated fabrication process, high cost, and narrow bandwidth prompt researchers to explore alternative SAs with novel materials [2]. Single-wall carbon nanotubes (CNTs) and two-dimensional (2D) layered materials including graphene and transition metal dichalcogenides (TMDCs) have been developed as SA candidates because of their ease of fabrication and much lower cost comparing with SESAMs [3–9]. 2D materials, in particular, are considered as potent prospects for the next-generation photonics technology because of their wideband responses and ultrafast carrier dynamics. However, graphene typically has a weak optical absorption (2.3% per layer) and TMDCs are more suitable in the visible due to their large bandgaps [10,11].

Quite recently, black phosphorus (BP), which is the most thermodynamically stable allotrope of phosphorus, has been re-discovered as a 2D material for optoelectronic applications [12].

Layered BP has a direct bandgap depending on the number of layers, 0.3 eV for bulk BP and 2 eV for monolayer BP. It thus has largely adjustable bandgaps and nonlinear absorption over a wide bandwidth [12]. Layered BP becomes a promising prospect in pulsed lasers in the infrared and mid-infrared region [13]. Q-switched and mode-locked pulsed fiber lasers triggered by BP-SAs have been presented in wavelengths ranging from 1 to 3  $\mu\text{m}$  [14–20]. However, the conventional method of fixating BP-SA in between the fiber end facets is far from an ideal approach [16,17]. Such-fabricated BP-SAs are easily exposed to a combination of oxygen and moisture in most environments. They are also vulnerable to optical damage when strong laser pulses are transmitting through. Therefore, it prompts an urgent study for an optimal BP-SA incorporation process for fiber lasers to assure better long-term stability and higher optical damage threshold.

Tapered fibers and side-polished D-shaped fibers have been developed for evanescent coupling between the light and 2D materials for passive Q-switching and mode-locking lasers [20–24]. The fiber taper approach is particularly promising for BP-SA incorporation for several reasons. First, when BP is deposited onto the side of the fiber tapers, it interacts with the evanescent field with a much larger active area. Compared with the conventional method of sandwiching BP between a pair of fiber facets [16,17], the material utilization efficiency is largely improved. Second, the optical damage threshold can be significantly enhanced due to the substantially reduced light intensity. Third, as the evanescent field and BP mostly interacts inside the innermost layers, it can effectively

\* Corresponding author at: School of Electronic and Optical Engineering, Nanjing University of Science and Technology, Nanjing 210094, China.

E-mail address: [lili@njust.edu.cn](mailto:lili@njust.edu.cn) (L. Li).

mitigate the environmental oxygen and moisture invasion. Eventually, it provides the possibility to completely isolate BP from the outer environment by depositing outer buffer layers.

In this paper, we report a passively Q-switched ytterbium-doped fiber laser (YDFL) employing a tapered-fiber-based BP-SA scheme with wavelength tunability, which has not been reported to date to the best of our knowledge. Few-layer BP was transferred onto the tapered fibers by an optically driven process. Utilizing an ytterbium-doped all-fiber ring cavity, passively Q-switched tunable laser emission was achieved. A Sagnac fiber loop [25,26] was used to provide the wavelength tuning ranging from 1040.5 to 1044.6 nm. The maximal average output power was 8.9 mW at a 63-kHz repetition rate and the maximal pulse energy was 141.27 nJ. The shortest pulse duration was 2.5 μs under 445-mW pump power. With BP-SA integrated onto the fiber tapers, these passively Q-switched fiber lasers can hold the benefits of enhancing laser-induced damage threshold and mitigating BP oxidation process to a large extent.

**Fabrication and optimization of tapered-fiber-based BP-SAs**

To prompt efficient interaction between the BP material and evanescent wave along the fiber tapers, a few critical challenges remain to be solved that include achieving optimal taper dimensions and high surface quality.

In our experiments, single-mode fibers (NUFERN, HI1060) were tapered down to a minimum of ~15 μm in diameter, as shown in Fig. 1(a). By shrinking the diameter, more evanescent wave couples with the surrounding materials; however, it also costs higher transmission loss and weaker mechanical strength. Tradeoff therefore has to be made regarding the optimal microfiber diameter and its length. In our experiments, we identified the best geometry to be a microfiber 15-μm in diameter and 1-mm in length by try and error with simulations.

Few-layer BP ethyl alcohol (EA) solution of a concentration of 0.5 mg/ml was utilized for BP-SA preparation. In the BP-EA solution, BP flakes were ~2 to 10 layers with lateral thickness of ~0.5 to 5 μm. To transfer BP flakes onto the fiber tapers, we adopted an optically driven (OD) method. With the tapered fibers fixed on top of a glass slide, we applied a few drops of solution onto the taper waists. At the same time, a continuous-wave laser power at 975 nm was transmitting through the fiber tapers for a few minutes. BP flakes could be deposited onto the taper side due to the combined effect of optical trapping force and heat convection. During this OD process, the enabling laser power level was also critical; otherwise, BP flakes would not be appropriately trapped onto the taper. The optimal laser power was found to be ~100

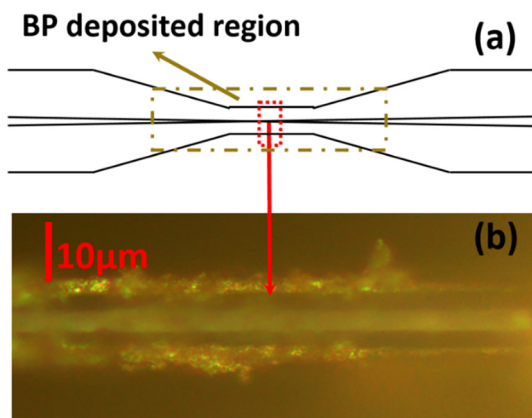


Fig. 1. (a) Tapered fiber illustration; (b) tapered fiber with BP deposited onto.

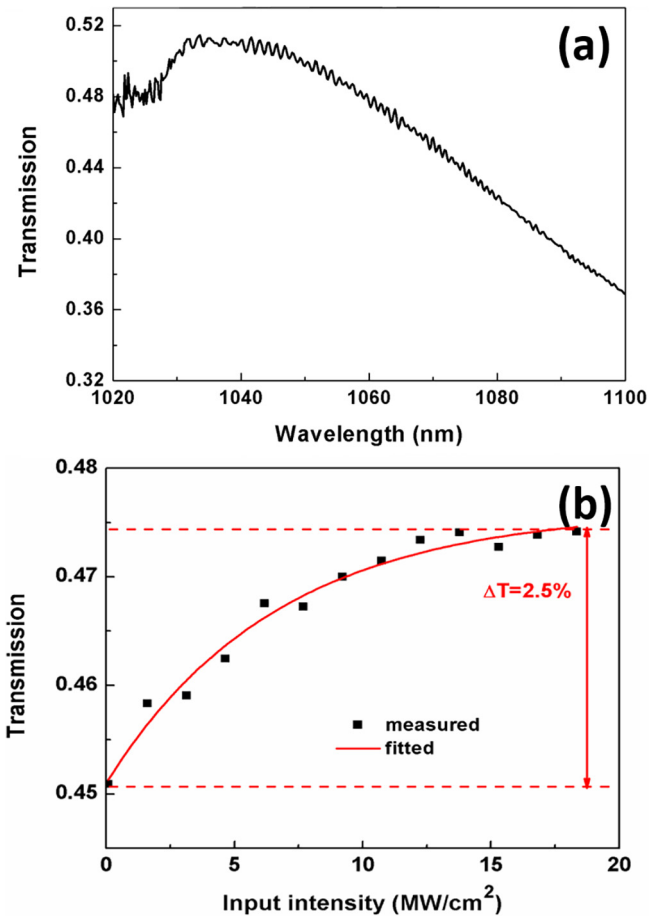


Fig. 2. (a) The transmission spectrum; (b) the saturable absorption of fabricated BP-SAs.

mW and the duration was ~15 min. Afterwards, the tapered fibers were air dried for about an hour. Compared with other methods of continuously dripping and air drying [14–17], the OD method possesses advantages of better repeatability and reliability. Fig. 1(a) illustrates the tapered microfiber and the BP deposition region; Fig. 1(b) is the microscopic image showing the micro-morphology of deposited BP.

To study transmission properties of the fabricated BP-SAs, we utilized a wideband 1-μm ASE light source (CONNET, VASS-Yb-B:

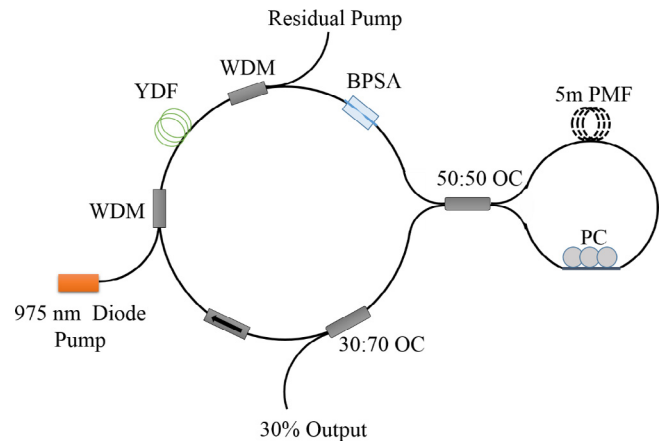


Fig. 3. The scheme of passively Q-switched BP-SA-based tunable all-fiber ring laser.

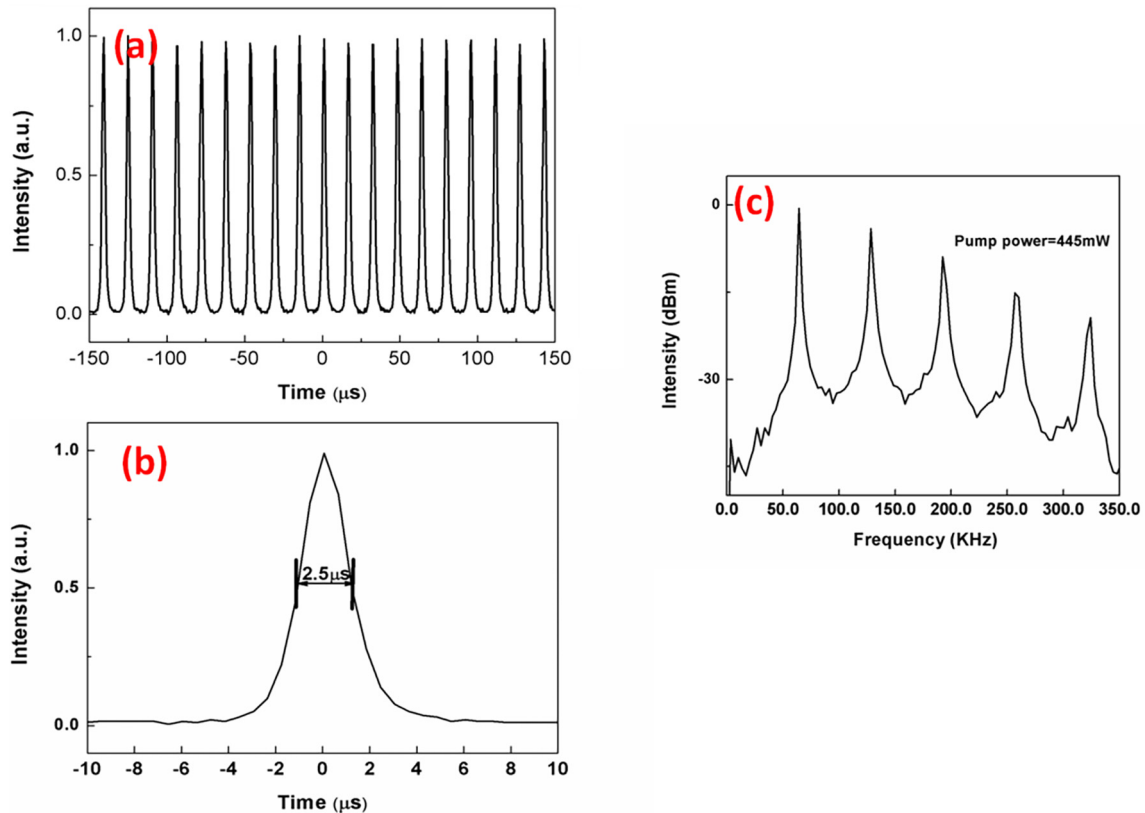


Fig. 4. (a) Q-switched laser pulse trains under 445 mW pump power; (b) single pulse envelope; (c) the RF spectrum.

SM) an optical spectrum analyzer (OSA, Anritsu, MS9710C) for spectrum analysis. Fig. 2(a) shows the transmission spectra of the tapered-fiber-based BP-SAs. The transmission is peaked at ~1035 nm and decreasing at longer wavelength up to 1100 nm. The transmission data is ~51% at the wavelength of 1040 nm.

We also used a homemade mode-locked fiber laser, which had a central wavelength of 1030 nm and a pulse duration of 6 ps at 52-MHz repetition rate, to measure the nonlinear absorption properties of the fabricated BP-SAs. The measurements are the dots shown in Fig. 2(b) and the solid curve is the fitted saturable absorption equation:

$$T(I) = 1 - \Delta T \exp\left(-\frac{1}{I_{sat}}\right) - T_{ns} \quad (1)$$

where  $\Delta T$  is the modulation depth,  $I_{sat}$  represents the saturable intensity, and  $T_{ns}$  is the non-saturable loss. From data fitting, the saturable intensity was 6.65 MW/cm<sup>2</sup>, the non-saturable absorption was 52.4%, and the modulation depth of the fabricated BP-SAs was ~2.5%.

### Construction of the passively Q-switched wavelength-tunable fiber laser

The tunable Yb-doped fiber (YDF) ring laser based on BP-SA is schematically shown in Fig. 3. A piece of 0.9-m-long YDF (NUFERN, SM-YSF-HI), whose absorption coefficient was 250 dB/m at 975 nm, was employed as the gain fiber. The YDF was pumped by a laser diode at 975 nm and the pump power was combined by a 975/1064 nm wavelength division multiplexer (WDM). A second WDM was inserted following the gain fiber to dump the residual pump. The BP-SA was spliced to the 1064-nm port of the second WDM. A Sagnac loop filter comprised of a 5-meter-long polarization maintaining fiber (PMF) and a polarization controller (PC)

was incorporated into the cavity for wavelength tuning [25,26]. A 30/70 single-mode output coupler (OC) was used for output power collection. A polarization-independent isolator (PI-ISO) was utilized to assure unidirectional propagation.

The output characteristics of the laser emissions were monitored by an OSA for spectral analysis, and an InGaAs photodetector (EOT et3000A, 2 GHz) with an oscilloscope (LeCroy Waverunner 625Zi, 2.5 GHz) for temporal measurement. The experimental results are presented in the next section.

### Wavelength-tunable pulsed laser performance and discussions

In the fiber laser experiments, stable Q-switched pulses were observed at a threshold pump power of ~220 mW. The initial rep-

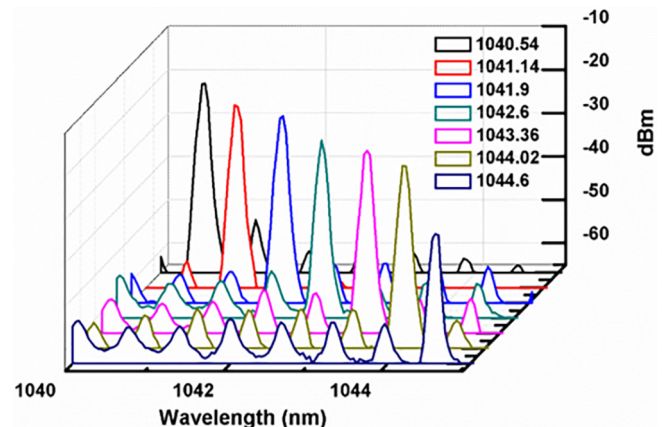


Fig. 5. Optical spectra of the tunable Q-switched fiber laser emissions.

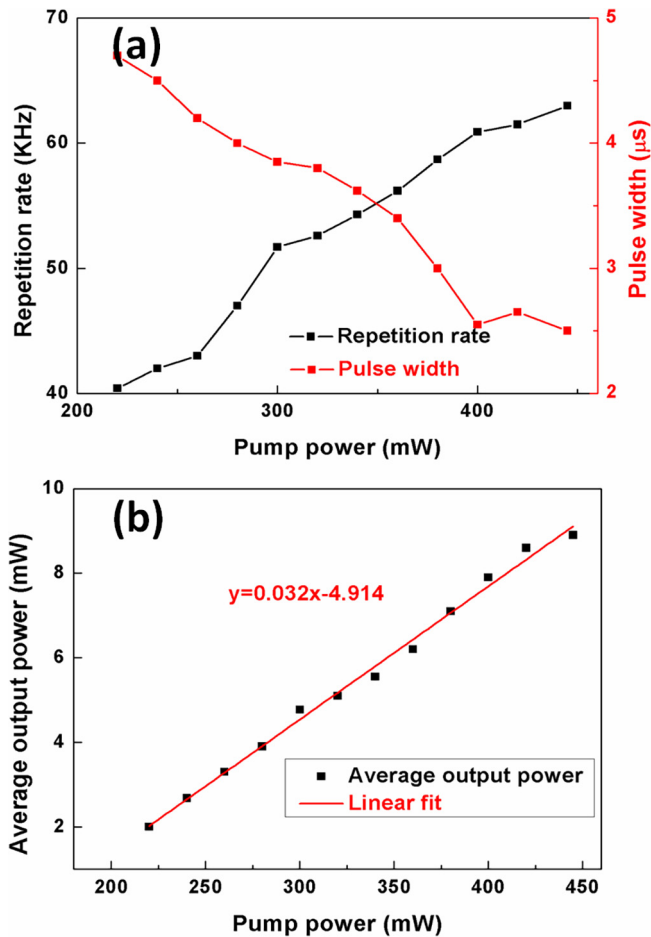


Fig. 6. (a) Repetition rate and pulse width vs. pump power. (b) Average output power vs. pump power.

etition rate was 40.4 kHz and pulse duration was 4.7  $\mu$ s. Robust laser pulses maintained up to 445 mW pump power and the repetition rate increased from 40.4 to 63 kHz. The Q-switched pulse trains at pump power of 445 mW are shown in Fig. 4(a). An enlarged pulse envelope indicating a 2.5- $\mu$ s pulse duration is shown in Fig. 4(b). Fig. 4(c) shows the radio-frequency (RF) spectrum of the Q-switched laser pulses, confirming the repetition rate of 63 kHz and a signal-to-noise ratio (SNR) of beyond 30 dB for the fundamental peak.

The wavelengths of the pulsed laser emission could be tuned from 1040.5 to 1044.6 nm by adjusting the PC in the Sagnac loop filter to change the polarization states. During the process of wavelength tuning, the variation of output power was less than 10%. The tuning spectra of laser emissions are presented in Fig. 5. The observed comb-like spectra are typical with high birefringence Sagnac fiber loops [25], and the primary emission peak is well over 30 dB in side-mode suppression ratio.

During the experiments, it was observed that the repetition rate of the laser pulses increased from 40.4 to 63 kHz and the pulse duration decreased from 4.7 to 2.5  $\mu$ s, when pump power increased from 220 to 445 mW, as shown in Fig. 6(a). Such observations agreed well with typical characteristics of passively Q-switched fiber lasers. Fig. 6(b) depicts the average output power versus pump power. The maximal average output power was 8.9 mW at 445 mW pump, and the pulse energy was 141.27 nJ, correspondingly. The relatively low slope efficiency of 3.2% was mainly caused by high cavity losses such as the insertion losses of BP-SA ( $\sim$ 3 dB), the Sagnac fiber loop, and the 30/70 output coupler.

To note, the Q-switched laser operation maintained robust under all pump power levels with no obvious pulse jitter or splitter observed. Regarding the stability of this tapered-fiber-based BP-SA all-fiber ring laser, we had activated and maintained non-stop laser emission for more than 6 h with no noticeable power variation and measurable spectrum shift. For its long-term stability and repeatability, this fiber laser had been running for an accumulated total of more than 100 h in a three-month span without any noticeable performance deterioration. Comparing with the previous pulsed 1- $\mu$ m fiber lasers utilizing BP-SA deposited onto fiber facets [14], the current approach was demonstrated to uphold better stability and repeatability for its inherently hermetic ability against environmental influence.

## Conclusion

To conclude, passively Q-switched wavelength-tunable 1- $\mu$ m all-fiber ring lasers utilizing tapered-fiber-based BP-SAs were demonstrated for the first time. The few-layer BP was deposited onto optimized fiber tapers with an OD process. The pump threshold of the Q-switched fiber lasers was  $\sim$ 220 mW and stable laser pulses maintained up to 445 mW pump power. The emission spectra were tunable from 1040.5 to 1044.6 nm by controlling the polarization states with a Sagnac fiber loop. Our experimental results suggested such tapered-fiber-based BP-SAs possessed better stability against the thermally prompted oxidation from the environment. Therefore, this approach could hold great prospects for BP-based pulsed fiber lasers in the near-infrared region.

## Acknowledgments

This work is supported by the High-Level Innovation and Entrepreneurship Talent Introduction Plan and the Educational Innovation Team Introduction Plan of Jiangsu Province, China, the National Natural Science Foundation of China (No. 61627802), and the Fundamental Research Funds for the Central Universities (No. 30916011103).

## References

- [1] Keller U, Weingarten KJ, Kartner FX, Kopf D, Braun B, Jung ID, Fluck R, Honninger C, Matuschek N, Aus der Au J. Semiconductor saturable absorber mirrors (SESAM's) for femtosecond to nanosecond pulse generation in solid-state laser. *IEEE J Sel Top Quantum Electron* 1996;2:435–53.
- [2] Keller U. Recent developments in compact ultrafast lasers. *Nature* 2003;424:831–8.
- [3] Woodward RI, Kelleher EJ. 2D saturable absorbers for fibre lasers. *Appl Sci* 2015;5:1440–56.
- [4] Set SY, Yaguchi H, Tanaka Y, Jablonski M. Ultrafast fiber pulsed lasers incorporating carbon nanotubes. *IEEE J Sel Top Quantum Electron* 2004;10:137–46.
- [5] Novoselov KS, Geim AK, Morozov SV, Jiang D, Zhang Y, Dubonos SV, Grigorieva IV, Firsov AA. Electric field effect in atomically thin carbon films. *Science* 2004;306:666–9.
- [6] Geim AK. Graphene: status and prospects. *Science* 2009;324:1530–4.
- [7] Ayari A, Cobas E, Ogundadegbe O, Fuhrer MS. Realization and electrical characterization of ultrathin crystals of layered transition-metal dichalcogenides. *J Appl Phys* 2007;101:014507.
- [8] Guo H, Feng M, Song F, Li H, Ren A, Wei X, Tian J. Q-Switched erbium-doped fiber laser based on silver nanoparticles as a saturable absorber. *IEEE Photon Technol Lett* 2016;28:135.
- [9] Ren A, Feng M, Song F, Ren Y, Yang S, Yang Z, Tian J. Actively Q-switched ytterbium-doped fiber laser by an all-optical Q-switcher based on graphene saturable absorber. *Opt Express* 2015;23:21490.
- [10] Wang QH, Kalantar-Zadeh K, Kis A, Coleman JN, Strano MS. Electronics and optoelectronics of two-dimensional transition metal dichalcogenides. *Nat Nanotechnol* 2012;7:699–712.
- [11] Wang K, Wang J, Fan J, Lotya M, O'Neill A, Fox D, Feng Y, Zhang X, Jiang B, Zhao Q, Zhang H, Coleman JN, Zhang L, Blau WJ. Ultrafast saturable absorption of two-dimensional MoS<sub>2</sub> nanosheets. *ACS Nano* 2013;7:9260–7.
- [12] Lu SB, Miao LL, Guo ZN, Qi X, Zhao CJ, Zhang H, Wen SC, Tang DY, Fan DY. Broadband nonlinear optical response in multi-layer black phosphorus: an

- emerging infrared and mid-infrared optical material. *Opt Express* 2015;23:11183–94.
- [13] Tran V, Soklaski R, Liang Y, Yang L. Layer-controlled band gap and anisotropic excitons in few-layer black phosphorus. *Phys Rev B* 2014;89:235319.
- [14] Song HQ, Wang Q, Zhang YF, Li L. Mode-locked ytterbium-doped all-fiber lasers based on few-layer black phosphorus saturable absorbers. *Opt Commun* 2017;394:157–60.
- [15] Kong LC, Qin ZP, Xie GQ, Guo ZN, Zhang H, Yuan P, Qian LJ. Black phosphorus as broadband saturable absorber for pulsed lasers from 1  $\mu\text{m}$  to 2.7  $\mu\text{m}$  wavelength. *Laser Phys Lett* 2016;13:045801.
- [16] Chen Y, Jiang G, Chen S, Guo Z, Yu X, Zhao C, Zhang H, Bao Q, Wen S, Tang D, Fan D. Mechanically exfoliated black phosphorus as a new saturable absorber for both Q-switching and Mode-locking laser operation. *Opt Express* 2015;23:12823–33.
- [17] Rashid FAA, Azzuhri SR, Salim MAM, Shaharuddin RA, Ismail MA, Ismail MF, Razak MZA, Ahmad H. Using a black phosphorus saturable absorber to generate dual wavelengths in a Q-switched ytterbium-doped fiber laser. *Laser Phys Lett* 2016;13:126201.
- [18] Luo ZC, Liu M, Guo ZN, Jiang XF, Luo AP, Zhao CJ, Yu XF, Xu WC, Zhang H. Microfiber-based few-layer black phosphorus saturable absorber for ultra-fast fiber laser. *Opt Express* 2015;23:20030–9.
- [19] Al-Masoodi AHH, Ahmed MHM, Latiff AA, Arof H, Harun SW. Q-switched ytterbium-doped fiber laser using black phosphorus as saturable absorber. *Chin Phys Lett* 2016;33:054206.
- [20] Huang KX, Lu BL, Li D, Qi XY, Chen HW, Wang JT, Bai. Black phosphorus flakes covered microfiber for Q-switched ytterbium-doped fiber laser. *Appl Opt* 2017;56:6427–31.
- [21] Wang J, Luo Z, Zhou M, Ye C, Fu H, Cai Z, Cheng H, Xu H, Qi W. Evanescent-light deposition of graphene onto tapered fibers for passive Q-switch and mode-locker. *IEEE Photon J* 2012;4:1295–305.
- [22] Du J, Wang Q, Jiang G, Xu C, Zhao C, Xiang Y, Chen Y, Wen S, Zhang H. Ytterbium-doped fiber laser passively mode locked by few-layer Molybdenum Disulfide (MoS<sub>2</sub>) saturable absorber functioned with evanescent field interaction. *Sci Rep* 2014;4:6346.
- [23] Mao D, Wang Y, Ma C, Han L, Jiang B, Gan X, Hua S, Zhang W, Mei T, Zhao J. WS<sub>2</sub> mode-locked ultrafast fiber laser. *Sci Rep* 2015;5:7965.
- [24] Liu S, Zhu X, Zhu G, Balakrishnan K, Zong J, Wiersma K, Peyghambarian N. Graphene Q-switched Ho<sup>3+</sup>-doped ZBLAN fiber laser at 1190 nm. *Opt Lett* 2015;40:147–50.
- [25] Ouyang C, Shum P, Wang H, Fu S, Cheng X, Wong JH, Tian X. Wavelength-tunable high-energy all-normal-dispersion Yb-doped mode-locked all-fiber laser with a HiBi fiber Sagnac loop filter. *IEEE J Quantum Electron* 2011;47:198–203.
- [26] Álvarez-Tamayo RI, Durán-Sánchez M, Pottiez O, Kuzin EA, Ibarra-Escamilla B, Flores-Rosas A. Theoretical and experimental analysis of tunable Sagnac high-birefringence loop filter for dual-wavelength laser application. *Appl Opt* 2011;50:253–60.